

Redox-responsive molecular helices with highly condensed π -clouds

Eisuke Ohta¹, Hiroyasu Sato², Shinji Ando¹, Atsuko Kosaka¹, Takanori Fukushima^{1*}, Daisuke Hashizume¹, Mikio Yamasaki³, Kimiko Hasegawa³, Azusa Muraoka⁴, Hiroshi Ushiyama⁴, Koichi Yamashita⁴ and Takuzo Aida^{1,2,5*}

Helices have long attracted the attention of chemists, both for their inherent chiral structure and their potential for applications such as the separation of chiral compounds or the construction of molecular machines. As a result of steric forces, polymeric *o*-phenylenes adopt a tight helical conformation in which the densely packed phenylene units create a highly condensed π -cloud. Here, we show an oligomeric *o*-phenylene that undergoes a redox-responsive dynamic motion. In solution, the helices undergo a rapid inversion. During crystallization, however, a chiral symmetry-breaking phenomenon is observed in which each crystal contains only one enantiomeric form. Crystals of both handedness are obtained, but in a non-racemic mixture. Furthermore, in solution, the dynamic motion of the helical oligomer is dramatically suppressed by one-electron oxidation. X-ray crystallography of both the neutral and oxidized forms indicated that a hole, generated upon oxidation, is shared by the repeating *o*-phenylene units. This enables conformational locking of the helix, and represents a long-lasting chiroptical memory.

Helical motifs play crucial roles in many biological functions. This notion has inspired chemists to design a wide variety of helical molecules¹, not only to investigate their inherent molecular chirality but also to use them for practical applications. For example, helical polymers with a high conformational stability have been used as separation media for optically active compounds^{2,3} and asymmetric catalysts^{4–7}. Dynamic molecular helices capable of responding to external stimuli by conformational changes can also serve as chiroptical sensors⁸ and actuators⁹. Examples of external stimuli that have been extensively studied so far include chiral compounds^{8,10–16}, solvents^{17,18}, metal ions^{9,19} and light^{20–23}. Redox-active helical polymers that change conformation in response to an electrochemical signal have been proposed to offer interesting potentials²⁴, but examples of such polymers are currently limited to polyisocyanides with redox-active units in their side chains^{25,26} that show a chiroptical response to oxidation.

In this Article, we describe a helix with a redox-active main chain that responds to electrical inputs by a conformational change. We first took note of an old work by Wittig and colleagues on the synthesis of oligomeric *o*-phenylenes^{27–29}. This molecular motif consists of multiple phenylene units that are linked together at their *ortho* positions (Fig. 1). Because of the heavily angled aromatic connection, polymeric *o*-phenylenes are forced to adopt a helical structure. In fact, a hexameric *o*-phenylene in the crystalline state was proven to form a one-handed 3_1 -helical conformation, in which three repeating monomeric units constitute a single helical pitch³⁰. However, it should be noted that oligomeric *o*-phenylenes, on oxidation, are easily subject to cyclization³¹, which has made their chemistry difficult to study. Here we demonstrate that this problem can be solved by nitration of the terminal aryl units. We

prepared the octameric *o*-phenylene OP8NO_2 (Fig. 1) and were able to show that it did not undergo oxidative cyclization. Moreover, we coincidentally noted that OP8NO_2 undergoes a chiral symmetry-breaking process during the purification process by recrystallization, affording enantiomerically pure crystals (Fig. 2). Crystals of both enantiomeric helices (right- and left-handed) are formed, but not in equal quantities, so the overall sample is not a racemic mixture. Finally, we show that the conformational rigidity of oligomeric *o*-phenylenes can be dramatically altered by electrical inputs (Fig. 2). In solution, the OP8NO_2 helices undergo rapid helical inversion. Following one-electron oxidation, however, they are converted into OP8NO_2^{+} helices, which adopt a more compact conformation and do not interconvert as easily, thus locking the helix into one conformation.

Results and discussion

Polyphenylene is one of the most fundamental π -conjugated architectures. In sharp contrast to the extensively studied *p*- and *m*-connected analogues^{9,32,33}, however, polymeric *o*-phenylenes have been recognized as an elusive class of π -conjugated compounds³⁴. Because they are difficult to synthesize, only a few reports on the preparation of short-chain *o*-phenylene oligomers^{30,31,35} have been made since the first synthetic trial by Wittig in 1957^{27–29}. Furthermore, their physical and chemical properties have largely remained unexplored. In the present work, we adopted an iterative synthetic method involving copper-mediated oxidative coupling of lithiated precursors. This method allowed for the incorporation of a variety of terminal functionalities, including Br (OP8Br), H (OP8H) and NO_2 (OP8NO_2) (Fig. 1). OP8Br can be converted into longer *o*-phenylenes that include 16, 24, 32, 40 and 48 aromatic

¹RIKEN Advanced Science Institute, 2-1 Hirosawa, Wako, Saitama 351-0198, Japan, ²Nanospace Project, Exploratory Research for Advanced Technology-Solution Oriented Research for Science and Technology (ERATO-SORST), Japan Science and Technology Agency, National Museum of Emerging Science and Innovation, 2-41 Aomi, Koto-ku, Tokyo 135-0064, Japan, ³Rigaku, 3-9-12 Matsubara-cho, Akishima, Tokyo 196-8666, Japan,

⁴Department of Chemical System Engineering, School of Engineering, The University of Tokyo, 7-3-1 Hongo, Bunkyo-ku, Tokyo 113-8656, Japan,

⁵Department of Chemistry and Biotechnology, School of Engineering, The University of Tokyo, 7-3-1 Hongo, Bunkyo-ku, Tokyo 113-8656, Japan.

*e-mail: fukushima@riken.jp; aida@macro.t.u-tokyo.ac.jp

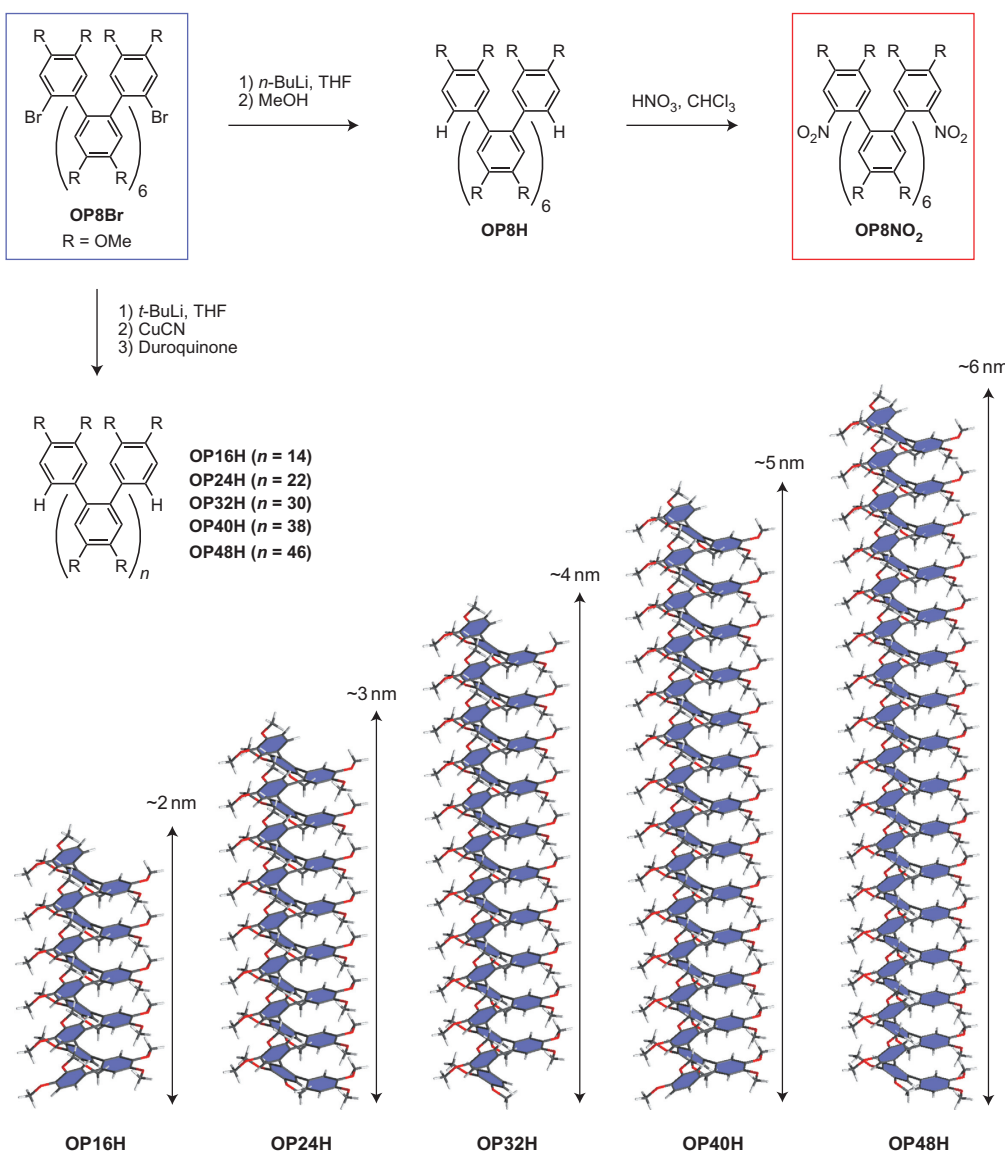


Figure 1 | Synthesis and schematic structures of OPnH ($n = 8, 16, 24, 32, 40$ and 48) and OP8NO₂. Top: synthesis of the *o*-phenylene oligomers OPnH from the brominated derivative OP8Br. Bottom: using the octameric oligomer as a precursor is crucial to obtain longer polymers that remain linear rather than undergoing cyclization.

rings (Fig. 1). We would like to emphasize here that the use of this octameric derivative as the precursor has been essential for obtaining such long *o*-phenylenes. When shorter-chain precursors such as the tetrameric homologue OP4Br were used (see Supplementary Information), the chain extension reaction was accompanied by an undesired intramolecular cyclization.

As described above, in an attempt to purify octameric *o*-phenylene derivatives OP8Br, OP8H and OP8NO₂ by recrystallization, we noticed that OP8NO₂ gives optically active single crystals (Fig. 2). Each of the crystals formed was pulverized by grinding with KBr. The resulting solid was moulded into a pellet and subjected to circular dichroism (CD) spectroscopy, which revealed a CD band at 265 nm (Fig. 3a). We initially thought that this observation could be explained by spontaneous optical resolution, which allows for the formation of single crystals consisting of either right-handed or left-handed enantiomers with equal probability. In a spontaneous optical resolution process, each single crystal is therefore optically active, but the whole system is a racemic mixture of the enantiomers and remains optically inactive.

However, a sample prepared by grinding together all the single crystals of OP8NO₂ formed in a single batch proved to be optically active (Fig. 4a). Furthermore, we observed that the optical purity was significantly enhanced when the crystallization was carried out with mechanical stirring (Fig. 4b). The intensity and sign of the CD spectra of the samples thus obtained changed every time, but the CD spectral features were very intense, sometimes even almost comparable (~98%) to those of single crystals of OP8NO₂. These chiroptical features clearly demonstrate the occurrence of chiral symmetry-breaking in the crystallization of OP8NO₂ and the formation of enantiomerically pure crystals, which can consist of either enantiomer. This parity-breaking event in crystallization, which leads to the emergence of optical activity, has long been a subject of particular interest in physics and has attracted attention in relation to the origin of homochirality in nature. However, rational understanding of this phenomenon still remains a challenge^{36–38}. Although several examples of ‘chiral symmetry-breaking’ have been reported^{39–41}, no molecular helices had so far been observed to undergo this parity-breaking event.

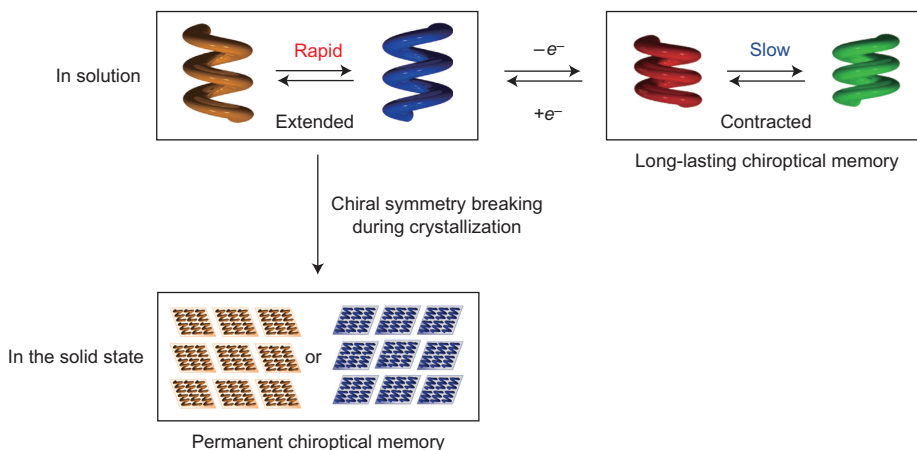


Figure 2 | Schematic representation of the helical inversion dynamics of OP8NO_2 in solution and in the solid state. Dynamically inverting OP8NO_2 crystallizes in either a right-handed (blue) or a left-handed helical form (orange) through chiral symmetry-breaking, affording crystals with a permanent chiroptical memory in the solid state (left, top to bottom panels). Although OP8NO_2 undergoes a rapid helical inversion in solution, this dynamic process becomes very slow after one-electron oxidation of the helices (green, right-handed; red, left-handed), thereby allowing OP8NO_2^{+} to acquire a long-lasting chiroptical memory (top, right and left panels).

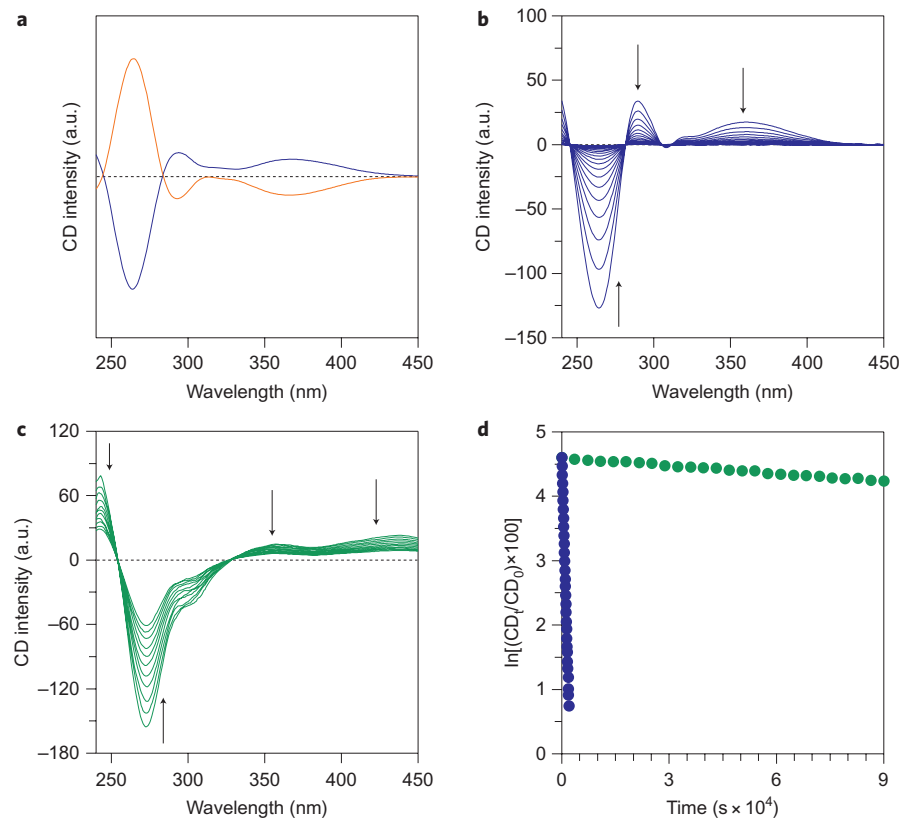


Figure 3 | Chiroptical features and helical inversion dynamics of the neutral and oxidized forms of OP8NO_2 . **a**, Circular dichroism (CD) spectra in a KBr pellet at 25 °C of single crystals of OP8NO_2 with right-handed (blue) and left-handed (orange) helical conformations (determined by X-ray crystallography). **b**, Time-dependent CD spectral change (135-s intervals) at -10 °C of a single crystal of OP8NO_2 dissolved in MeCN. **c**, Time-dependent CD spectral change (6-h intervals) at -10 °C of a single crystal of OP8NO_2 dissolved in MeCN in the presence of the one-electron oxidant $(4\text{-BrC}_6\text{H}_4)_3\text{N}^{+}\text{[SbCl}_6^{-}]$. The black arrows in **b** and **c** represent the evolution of the CD intensities over time. **d**, Decay profiles of the CD intensities at 265 and 273 nm in spectra **b** (blue) and **c** (green), respectively. The linear decay profiles indicate that the racemization events of OP8NO_2 and its oxidized form follow a first-order kinetics, where the helical inversion rates (k_{inv}) at -10 °C are determined as 9.84×10^{-4} and $2.18 \times 10^{-6} \text{ s}^{-1}$ in the absence and presence of the oxidant, shown in blue and green, respectively.

Under optimized conditions, yellow-coloured prismatic crystals suitable for X-ray crystallography were obtained. The crystals have a chiral space group C2, where OP8NO_2 adopts a perfect

3₁-helical conformation (Fig. 5a,b) with interplanar distances between the cofacially oriented phenylene units of 3.232–3.285 Å (Fig. 5c). For comparison, we note that these values are much

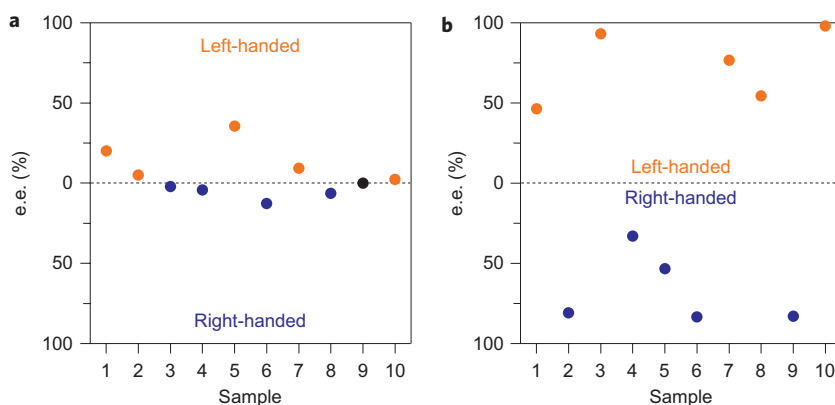


Figure 4 | Chiral symmetry-breaking in the crystallization of OP8NO_2 . **a,b**, Helical handedness data and enantiomeric excess (e.e.) values of various samples of OP8NO_2 crystals formed upon recrystallization from MeCN without (**a**) and with (**b**) mechanical stirring. Each dot represents a different single batch. Sample 9 (black dot) did not show any CD signal. We observe that chiral symmetry-breaking is enhanced by mechanical stirring.

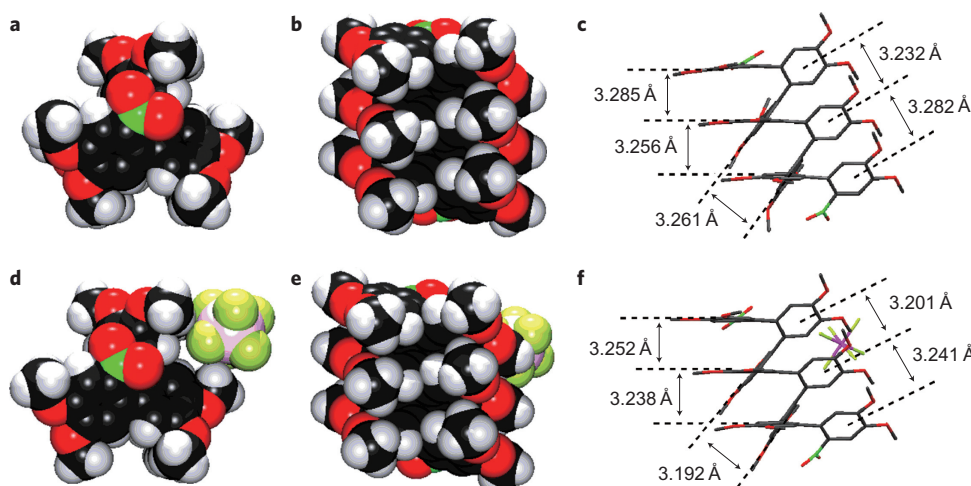


Figure 5 | Crystal structures of OP8NO_2 and $\text{OP8NO}_2^{\bullet+}[\text{SbF}_6^-]$ adopting a heavily twisted 3_1 -helical structure. **a-c**, Top view (**a**) and side view (**b**) of OP8NO_2 with interplanar distances between cofacially oriented phenylene units (**c**). For comparison, the observed distances are much shorter than the intersheet distance of graphite (3.35 Å). **d-f**, Top view (**d**) and side view (**e**) of $\text{OP8NO}_2^{\bullet+}[\text{SbF}_6^-]$ with interplanar distances between cofacially oriented phenylene units (**f**). The observed distances are noticeably shorter than those for OP8NO_2 due to a decrease in π -electronic repulsion, so that the interconversion between helices of opposite handedness is much slower.

shorter than the intersheet distance of graphite (3.35 Å). When viewed along the longer axis of the molecule, the proximal phenylene units overlap with one another almost perfectly. As shown by a crystal packing diagram (Supplementary Fig. S4b), a single crystal consists exclusively of the right-handed or left-handed helical conformer of OP8NO_2 . The crystallographic data (see Supplementary Information) allowed us to confirm that a single crystal composed of the right-handed helical conformer of OP8NO_2 shows a negatively signed Cotton effect at 265 nm (Fig. 3a; blue). As expected, a CD spectrum that is a perfect mirror image to the above was observed for a single crystal consisting of the left-handed helical conformer (Fig. 3a; orange).

The single crystals of OP8NO_2 , upon heating, remained optically up to its phase transition temperature at 191 °C (Supplementary Fig. S6), indicating a high conformational stability of OP8NO_2 in the crystal lattice. However, once the crystals were dissolved in acetonitrile (MeCN) at 25 °C, the characteristic optical activity disappeared almost instantaneously, indicating the occurrence of a rapid helical inversion in solution. The helical inversion took place even at -10 °C in MeCN, where the half-life ($t_{1/2}$) of the CD intensity at 265 nm was only 352 s (Fig. 3b). The time-dependent CD spectral change thus observed obeyed a first-order

kinetics with a rate constant of $9.84 \times 10^{-4} \text{ s}^{-1}$ (Fig. 3d; blue). A detailed kinetic analysis at different temperatures revealed that the activation energy for the helical inversion of OP8NO_2 is 88.3 kJ mol⁻¹ (Supplementary Fig. S9a).

Before the exploration of its redox-responsive conformational behaviour, we investigated the electrochemical properties of helical OP8NO_2 . In cyclic voltammetry (CV), OP8NO_2 showed a substantial stability against oxidation and released up to four electrons at +0.62, +0.82, +1.01 and +1.22 V (versus Ag/Ag⁺, in MeCN) in a stepwise manner. The resulting multiply oxidized species in turn accepted electrons to revert to its neutral form (Supplementary Fig. S7). Encouraged by this unusual electrochemical stability, we attempted to oxidize OP8NO_2 using a one-electron oxidant such as tris(4-bromophenyl)ammonium hexachloroantimonate [$(4\text{-BrC}_6\text{H}_4)_3\text{N}^{\bullet+}[\text{SbCl}_6^-]$]. We pulverized a single crystal of OP8NO_2 and added the resulting powder at -20 °C to an MeCN solution of $(4\text{-BrC}_6\text{H}_4)_3\text{N}^{\bullet+}[\text{SbCl}_6^-]$, whereupon an instantaneous colour change from yellow to green took place. Electron spin resonance (ESR) spectroscopy of the resulting solution showed a single broad line (Supplementary Fig. S2), indicating the formation of a radical cation of OP8NO_2 ($\text{OP8NO}_2^{\bullet+}$). This solution was CD active, with a partly different spectral pattern from that of neutral

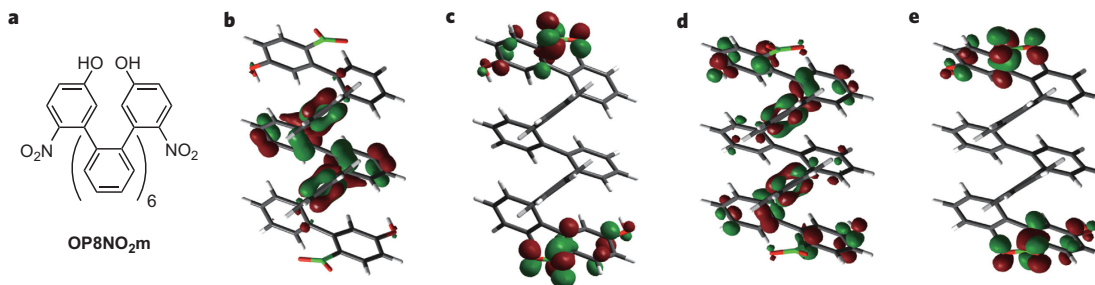


Figure 6 | Density functional theory (DFT) calculation of a model compound of OP8NO_2 ($\text{OP8NO}_2\text{m}$) at the B3LYP/6-31G(d) level. **a**, Molecular structure of $\text{OP8NO}_2\text{m}$. **b,c**, An optimized geometry of the neutral form of $\text{OP8NO}_2\text{m}$ with its highest occupied molecular orbital (HOMO; **b**) and lowest unoccupied molecular orbital (LUMO; **c**). **d,e**, Optimized geometry of the one-electron oxidized form (radical cation) of $\text{OP8NO}_2\text{m}$ with its singly occupied molecular orbital (SOMO; **d**) and LUMO (**e**). These orbitals are drawn with an isosurface value of 0.04. The oxidized form of $\text{OP8NO}_2\text{m}$ adopts a more compact conformation, where a hole generated in the molecule distributes at the outer six phenylene units. For **b–e**: grey, C; white, H; green, N; red: O.

OP8NO_2 (Fig. 3c). Of particular interest was the fact that the optical activity lasted for a very long period of time (Fig. 3d; green); the half-life at -10°C ($t_{1/2} = 44$ h), for example, was 450 times as long as that observed for neutral OP8NO_2 ($t_{1/2} = 352$ s at -10°C , *vide ante*) (Fig. 3d; blue). Again, the racemization profile followed a first-order kinetics with a rate constant at -10°C of $2.18 \times 10^{-6}\text{ s}^{-1}$, where the activation energy for the helical inversion of $\text{OP8NO}_2^{\bullet+}$ was evaluated as 96.6 kJ mol^{-1} (Supplementary Fig. S9b). This value is higher by 8.3 kJ mol^{-1} than that of its neutral form.

We also succeeded in obtaining the crystal structure of one-electron oxidized $\text{OP8NO}_2^{\bullet+}$. When ether vapour was allowed to diffuse at 25°C into an MeCN solution of $\text{OP8NO}_2^{\bullet+}[\text{SbF}_6^-]$, once isolated from the reaction mixture of OP8NO_2 and $\text{NO}^{\bullet+}[\text{SbF}_6^-]$, single crystals suitable for X-ray crystallography formed. As is clearly shown in Fig. 5d,e, OP8NO_2 , on oxidation, was able to preserve its 3_1 -helical conformation. Importantly, the observed interplanar distances between the proximal phenylene units (3.192 – 3.252 \AA , Fig. 5f) in one-electron oxidized $\text{OP8NO}_2^{\bullet+}$ are 0.02 – 0.07 \AA shorter than those of the neutral form of OP8NO_2 (Fig. 5c). We also noticed that all the C–O bonds in $\text{OP8NO}_2^{\bullet+}$ (1.340 – 1.365 \AA) are noticeably shorter than the corresponding bonds in the neutral form (1.358 – 1.381 \AA) (Supplementary Table S1). The structural characteristics thus observed for $\text{OP8NO}_2^{\bullet+}$ allowed us to conclude that a hole, generated by one-electron oxidation, is delocalized extensively over the helically twisted π -electronic array.

The geometrical shrinkage of OP8NO_2 on oxidation was supported by a theoretical calculation of its simplified model $\text{OP8NO}_2\text{m}$ (Fig. 6a) using density functional theory (DFT) at the B3LYP/6-31G(d) level. Figure 6b,c shows the highest occupied molecular orbital (HOMO) and lowest unoccupied molecular orbital (LUMO) distributions, respectively. This optimized structure of $\text{OP8NO}_2\text{m}$ clearly showed that its neutral form adopts a 3_1 -helical conformation, with a helical pitch of 4.35 \AA (that is, the average centre-to-centre distance between the proximal phenylene units). We also calculated one-electron oxidized $\text{OP8NO}_2\text{m}^{\bullet+}$ and found that it adopts a 3_1 -helical conformation with a reduced helical pitch of 3.95 \AA (Fig. 6d,e). Therefore, the geometrical shrinkage of OP8NO_2 on oxidation, as observed crystallographically, may not be attributable to the effect of crystal packing, but is most probably an intrinsic feature of the molecule. Although the HOMO of optimized $\text{OP8NO}_2\text{m}$ is localized on the four internal phenylene units (Fig. 6b), the SOMO (singly occupied molecular orbital) of $\text{OP8NO}_2\text{m}^{\bullet+}$ distributes at the outer six phenylene units (Fig. 6d). This result supports the suggestion from the crystal structure of $\text{OP8NO}_2^{\bullet+}$ that a hole, generated in the molecule by the removal of one electron, is shared by the repeating *o*-phenylene units.

Overall, we can conclude that the oxidized form of helical OP8NO_2 is conformationally locked by an attractive force operating among the densely packed phenylene units (Fig. 2). On removal of

electrons, a repulsive interaction that operates between condensed π -clouds⁴² can be reduced, or can even become attractive^{43–50}. This is a fundamental subject of molecular science and has been well documented in cofacially assembled noncovalent and covalent π -systems. However, these studies highlight only the static aspect of π -bonding interactions. In contrast, through investigations on the conformational change of an electrochemically stable oligomeric *o*-phenylene (OP8NO_2) with helically condensed π -clouds, the present work sheds light on the dynamic aspect of π -bonding.

Methods

Spontaneous symmetry breaking of OP8NO_2 in crystallization. An MeCN solution (5 ml) of OP8NO_2 (30 mg, 25 μmol) was refluxed for 2 h, then allowed to cool to 25°C . The resulting solution was filtered with a polytetrafluoroethylene membrane, and the filtrate was divided into five samples of 1 ml each and allowed to stand. After 24 h, the formed crystals were thoroughly collected by filtration and dried under reduced pressure. The crystals were then pulverized by grinding, and a small portion (0.1–0.2 mg) of the resulting powder was pressed with KBr powder (100–150 mg) into a transparent pellet, which was subjected to CD spectroscopy. Following the CD spectral measurement, the pellet was dissolved in a mixture of MeCN and water (5 ml; 1:1 v/v), and the resulting solution was subjected to electronic absorption spectroscopy. The exact amount of OP8NO_2 in the pellet was quantified by an absorbance at 290 nm. The e.e. value for all the crystals (Fig. 4a) was determined on the basis of a calibration curve (Supplementary Fig. S8), given by a correlation between the CD intensity and absorbance of single-crystalline OP8NO_2 (100% e.e.). Similarly, e.e. values of crystalline OP8NO_2 samples, isolated by recrystallization under mechanical stirring, were determined (Fig. 4b). For sample preparation, an MeCN solution (10 ml) of OP8NO_2 (59 mg, 50 μmol) was refluxed for 2 h while stirring using a magnetic stirrer bar. The resulting solution was allowed to cool to 25°C with continuous stirring. After 2 h, the microcrystals that were precipitated were corrected by filtration and dried under reduced pressure.

Kinetic study on helical inversion of OP8NO_2 . An arbitrarily chosen single crystal of OP8NO_2 was pulverized and dissolved in MeCN (3.5 ml) at a given temperature, and the resulting solution was immediately subjected to CD spectroscopy at the same temperature. For the preparation of its one-electron oxidized form ($\text{OP8NO}_2^{\bullet+}$), a single crystal of OP8NO_2 was pulverized and dissolved in MeCN solution (3.5 ml) containing an excess amount of $(4\text{-BrC}_6\text{H}_4)_3\text{N}^{\bullet+}[\text{SbCl}_6^-]$ (typically 0.4 mg), and the resulting mixture was also subjected to CD spectroscopy. The observed decay profiles of OP8NO_2 and $\text{OP8NO}_2^{\bullet+}$ both satisfied first-order kinetics, where the rate constants of racemization (k_{rac}) and helical inversion (k_{inv}) were obtained from equation (1):

$$\ln[(\text{CD}_t/\text{CD}_0) \times 100] = -k_{\text{rac}}t = -2k_{\text{inv}}t \quad (1)$$

The half-life ($t_{1/2}$) of the CD intensity was obtained from equation (2):

$$t_{1/2} = \ln 2/k_{\text{rac}} = \ln 2/2k_{\text{inv}} = 0.693/2k_{\text{inv}} \quad (2)$$

The k_{inv} values obtained at various temperatures were plotted (Supplementary Fig. S9a,b) and analysed according to the Arrhenius equation (3):

$$\ln k_{\text{inv}} = \ln A - E_a/RT \quad (3)$$

where A , E_a , R and T are frequency factor, activation energy, gas constant and absolute temperature, respectively.

Received 23 June 2010; accepted 6 October 2010;
published online 14 November 2010

References

- Yashima, E., Maeda, K., Iida, H., Furusho, Y. & Nagai, K. Helical polymers: synthesis, structures, and functions. *Chem. Rev.* **109**, 6102–6211 (2009).
- Yuki, H., Okamoto, Y. & Okamoto, I. Resolution of racemic compounds by optically active poly(triphenylmethyl methacrylate). *J. Am. Chem. Soc.* **102**, 6356–6358 (1980).
- Okamoto, Y. Chiral polymers for resolution of enantiomers. *J. Polym. Sci. A* **47**, 1731–1739 (2009).
- Yashima, E., Maeda, Y. & Okamoto, Y. Synthesis of poly[N-(4-ethynylbenzyl) ephedrine] and its use as a polymeric catalyst for enantioselective addition of dialkylzincs to benzaldehyde. *Polym. J.* **31**, 1033–1036 (1999).
- Reggelin, M., Doerr, S., Klussmann, M., Schultz, M. & Holzbach, M. Helically chiral polymers: a class of ligands for asymmetric catalysis. *Proc. Natl Acad. Sci. USA* **101**, 5461–5466 (2004).
- Roelfes, G. & Feringa, B. L. DNA-based asymmetric catalysis. *Angew. Chem. Int. Ed.* **44**, 3230–3232 (2005).
- Yamamoto, T. & Sugino, M. Helical poly(quinoxaline-2,3-diylyls) bearing metal-binding sites as polymer-based chiral ligands for asymmetric catalysis. *Angew. Chem. Int. Ed.* **48**, 539–542 (2009).
- Yashima, E. & Maeda, K. Chirality-responsive helical polymers. *Macromolecules* **41**, 3–12 (2008).
- Miwa, K., Furusho, Y. & Yashima, E. Ion-triggered spring-like motion of a double helicate accompanied by anisotropic twisting. *Nature Chem.* **2**, 444–449 (2010).
- Green, M. M. *et al.* A helical polymer with a cooperative response to chiral information. *Science* **268**, 1860–1866 (1995).
- Yashima, E., Matsushima, T. & Okamoto, Y. Poly((4-carboxyphenyl)acetylene) as a probe for chirality assignment of amines by circular dichroism. *J. Am. Chem. Soc.* **117**, 11596–11597 (1995).
- Prince, R. B., Barnes, S. A. & Moore, J. S. Foldamer-based molecular recognition. *J. Am. Chem. Soc.* **112**, 2758–2762 (2000).
- Waki, M., Abe, H. & Inouye, M. Translation of mutarotation into induced CD signals through helix inversion of host polymers. *Angew. Chem. Int. Ed.* **46**, 3059–3061 (2007).
- Petitjean, A., Nierengarten, H., van Dorsselaer, A. & Lehn, J.-M. Self-organization of oligomeric helical stacks controlled by substrate binding in a tobacco mosaic virus like self-assembly process. *Angew. Chem. Int. Ed.* **43**, 3695–3699 (2004).
- Hou, J.-L. *et al.* Hydrogen bonded oligohydrazide foldamers and their recognition for saccharides. *J. Am. Chem. Soc.* **126**, 12386–12394 (2004).
- Maurizot, V., Dolain, C. & Huc, I. Intramolecular versus intermolecular induction of helical handedness in pyridinedicarboxamide oligomers. *Eur. J. Org. Chem.* **2005**, 1293–1301 (2005).
- Okoshi, K., Sakurai, S.-I., Ohsawa, S., Kumaki, J. & Yashima, E. Control of main-chain stiffness of a helical poly(phenylacetylene) by switching on and off the intramolecular hydrogen bonding through macromolecular helicity inversion. *Angew. Chem. Int. Ed.* **45**, 8173–8176 (2006).
- Yamamoto, T., Yamada, T., Nagata, Y. & Sugino, M. High-molecular-weight polyquinoxaline-based helically chiral phosphine (PQXphos) as chirality-switchable, reusable, and highly enantioselective monodentate ligand in catalytic asymmetric hydrosilylation of styrenes. *J. Am. Chem. Soc.* **132**, 7899–7901 (2010).
- Kim, H.-J., Lee, E., Park, H.-S. & Lee, M. Dynamic extension–contraction motion in supramolecular springs. *J. Am. Chem. Soc.* **129**, 10994–10995 (2007).
- Maxein, G. & Zentel, R. Photochemical inversion of the helical twist sense in chiral polyisocyanates. *Macromolecules* **28**, 8438–8440 (1995).
- Li, J., Schuster, G. B., Cheon, K.-S., Green, M. M. & Selinger, J. V. Switching a helical polymer between mirror images using circularly polarized light. *J. Am. Chem. Soc.* **122**, 2603–2612 (2000).
- Pijper, D. & Feringa, B. L. Molecular transmission: controlling the twist sense of a helical polymer with a single light-driven molecular motor. *Angew. Chem. Int. Ed.* **46**, 3693–3696 (2007).
- King, E. D., Tao, P., Sanan, T. T., Hadad, C. M. & Parquette, J. R. Photomodulated chiral induction in helical azobenzene oligomers. *Org. Lett.* **10**, 1671–1674 (2008).
- Marsella, M. J., Rahbarinia, S. & Wilmot, N. Molecular springs, muscles, rheostats, and precessing gyroscopes: from review to preview. *Org. Biomol. Chem.* **5**, 391–400 (2007).
- Hida, N. *et al.* Helical, chiral polyisocyanides bearing ferrocenyl groups as pendants: synthesis and properties. *Angew. Chem. Int. Ed.* **42**, 4349–4352 (2003).
- Gomar-Nadal, E., Veciana, J., Rovira, C. & Amabilino, D. B. Chiral teleinduction in the formation of a macromolecular multistate chiroptical redox switch. *Adv. Mater.* **17**, 2095–2098 (2005).
- Wittig, G. & Lehmann, G. Über die Reaktionsweise von 2,2'-Dilithium-diphenyl gegenüber Metallchloriden; Gleichzeitig ein Beitrag zur Synthese von Poly-*o*-phenylenen. *Chem. Ber.* **90**, 875–892 (1957).
- Winkler, H. J. S. & Wittig, G. Preparation and reactions of *o*-dilithiobenzene. *J. Org. Chem.* **28**, 1733–1740 (1963).
- Wittig, G. & Klar, G. Über die Reaktionsweise von 2,2'-Dilithium-biphenyl gegenüber Metallhalogeniden, II. *Liebigs Ann. Chem.* **704**, 91–108 (1967).
- Blake, A. J., Cooke, P. A., Doyle, K. J., Gair, S. & Simpkins, N. S. Poly-*o*-phenylenes: synthesis by Suzuki coupling and solid state helical structures. *Tetrahedron Lett.* **39**, 9093–9096 (1998).
- Ormsby, J. L., Black, T. D., Hilton, C. L., Bharat & King, B. T. Rearrangements in the Scholl oxidation: implications for molecular architectures. *Tetrahedron* **64**, 11370–11378 (2008).
- Geerts, Y., Klärner, G. & Müllen, K. *Electronic Materials: The Oligomer Approach* Ch. 1 (Wiley-VCH, 1998).
- Goto, H., Furusho, Y., Miwa, K. & Yashima, E. Double helix formation of oligoresorcinols in water: thermodynamic and kinetic aspects. *J. Am. Chem. Soc.* **131**, 4710–4719 (2009).
- Voisin, E. & Williams, V. E. Do catechol derivatives electropolymerize? *Macromolecules* **41**, 2994–2997 (2008).
- Ibuki, E., Ozasa, S. & Murai, K. Studies of polyphenyls and polyphenylenes. I. The syntheses and infrared and electronic spectra of several sexiphenyls. *Bull. Chem. Soc. Jpn.* **48**, 1868–1874 (1975).
- Viedma, C. Chiral symmetry breaking during crystallization: complete chiral purity induced by nonlinear autocatalysis and recycling. *Phys. Rev. Lett.* **94**, 065504 (2005).
- Noorduin, W. L., Vlieg, E., Kellogg, R. M. & Kaptein, B. From Ostwald ripening to single chirality. *Angew. Chem. Int. Ed.* **48**, 9600–9606 (2009).
- Uwaha, M. & Katsuno, H. Mechanism of chirality conversion by grinding crystals: Ostwald ripening vs crystallization of chiral clusters. *J. Phys. Soc. Jpn.* **78**, 023601 (2009).
- Kondepudi, D. K., Kaufman, R. J. & Singh, N. Chiral symmetry breaking in sodium chloride crystallization. *Science* **250**, 975–976 (1990).
- Kondepudi, D. K. & Asakura, K. Chiral autocatalysis, spontaneous symmetry breaking, and stochastic behavior. *Acc. Chem. Res.* **34**, 946–954 (2001).
- Sakamoto, M. *et al.* Breaking the symmetry of axially chiral N-aryl-2(1H)-pyrimidinones by spontaneous crystallization. *Angew. Chem. Int. Ed.* **42**, 4360–4363 (2003).
- Hunter, C. A. & Sanders, J. K. M. The nature of π – π interactions. *J. Am. Chem. Soc.* **112**, 5525–5534 (1990).
- Milosevich, S. A., Saichek, K., Hinchen, L., England, W. B. & Kovacic, P. Coordination in benzene dimer cation radical. *J. Am. Chem. Soc.* **105**, 1088–1090 (1983).
- Hiraoka, K., Fujimaki, S., Aruga, K. & Yamabe, S. Stability and structure of benzene dimer cation $(C_6H_6)_2^+$ in the gas phase. *J. Chem. Phys.* **95**, 8413–8418 (1991).
- Graf, D. D., Duan, R. G., Campbell, J. P., Miller, L. L. & Mann, K. R. From monomers to π -stacks. A comprehensive study of the structure and properties of monomeric, π -dimerized, and π -stacked forms of the cation radical of 3',4'-dibutyl-2,5'-diphenyl-2,2':5',2"-terthiophene. *J. Am. Chem. Soc.* **119**, 5888–5899 (1997).
- Itagaki, Y., Benetics, N. P., Kadam, R. M. & Lund, A. Structure of dimeric radical cations of benzene and toluene in halocarbon matrices: An EPR, ENDOR and MO study. *Phys. Chem. Chem. Phys.* **2**, 2683–2689 (2000).
- Yamazaki, D., Nishinaga, T., Tanino, N. & Komatsu, K. Terthiophene radical cations end-capped by bicyclo[2.2.2]octane units: formation of bent π -dimers mutually attracted at the central position. *J. Am. Chem. Soc.* **128**, 14470–14471 (2006).
- Song, C. & Swager, T. M. π -Dimer formation as the driving force for calix[4]arene-based molecular actuators. *Org. Lett.* **10**, 3575–3578 (2008).
- Chebny, V. J., Shukla, R., Lindeman, S. V. & Rathore, R. Molecular actuator: redox-controlled clam-like motion in a bichromophoric electron donor. *Org. Lett.* **11**, 1939–1942 (2009).
- Das, T. N. Monomer and dimer radical cations of benzene, toluene, and naphthalene. *J. Phys. Chem. A* **113**, 6489–6493 (2009).

Acknowledgements

This work was supported by KAKENHI (21350108). The authors thank S. Ohkoshi and K. Nakabayashi (University of Tokyo) for the measurement of the ESR spectrum.

Author contributions

T.F. and T.A. designed the work. E.O., T.F. and T.A. wrote the paper. E.O., H.S., S.A. and A.K. performed the experiments. Single-crystal X-ray diffraction studies were carried out through the collaboration of D.H., M.Y. and K.H., A.M., H.U. and K.Y. were responsible for DFT calculations.

Additional information

The authors declare no competing financial interests. Supplementary information and chemical compound information accompany this paper at www.nature.com/naturechemistry. Reprints and permission information is available online at <http://npg.nature.com/reprintsandpermissions/>. Correspondence and requests for materials should be addressed to T.F. and T.A.